Nitrite and nitric oxide are important in the adjustment of primary metabolism during the hypersensitive response in tobacco

Mur, Luis; Kumari, Aprajita; Brotman, Yariv; Zeier, Jürgen; Mandon, Julian; Cristescu, Simona M.; Harren, Frans; Kaiser, Werner ; Fernie, Alisdair R.; Gupta, Kapuganti Jagadis

Published in:
Journal of Experimental Botany

DOI:
10.1093/jxb/erz161

Publication date:
2019

Citation for published version (APA):
Mur, L., Kumari, A., Brotman, Y., Zeier, J., Mandon, J., Cristescu, S. M., Harren, F., Kaiser, W., Fernie, A. R., & Gupta, K. J. (2019). Nitrite and nitric oxide are important in the adjustment of primary metabolism during the hypersensitive response in tobacco. *Journal of Experimental Botany*, *70*(17), 4571-4582. https://doi.org/10.1093/jxb/erz161

Journal of Experimental Botany
doi:10.1093/jxb/erz161 Advance Access Publication 10 April 2019
This paper is available online free of all access charges (see https://academic.oup.com/jxb/pages/openaccess for further details)

RESEARCH PAPER

Nitrite and nitric oxide are important in the adjustment of primary metabolism during the hypersensitive response in tobacco

Luis A. J. Mur[2], Aprajita Kumari[1], Yariv Brotman[3], Jurgen Zeier[4], Julien Mandon[5], Simona M. Cristescu[5], Frans Harren[5], Werner M. Kaiser[6], Alisdair R. Fernie[3] and Kapuganti Jagadis Gupta[1,*],

[1] National Institute of Plant Genome Research, Aruna Asaf Ali Marg, 110067, New Delhi, India
[2] Institute of Environmental and Rural Science, Aberystwyth University, Edward Llwyd Building, Aberystwyth, SY23 3DA, UK
[3] Max-Planck-Institute of Molecular Plant Physiology, Am Mühlenberg 1, D-14476 Golm-Potsdam, Germany
[4] Institute of Plant Molecular Ecophysiology, Heinrich-Heine-Universität Universitätsstrasse, 1 40225 Düsseldorf, Germany
[5] Radboud University, Life Science Trace Gas Facility, Molecular and Laser Physics, Institute for Molecules and Materials, PO Box 9010, 6500 GL Nijmegen, The Netherlands
[6] Julius-von-Sachs-Institut für Biowissenschaften; Lehrstuhl für Molekulare Pflanzenphysiologie und Biophysik; Julius-von-Sachs-Platz 2; D-97082 Wuerzburg, Germany

* Correspondence: jgk@nipgr.ac.in

Received 17 December 2018; Editorial decision 28 March 2019; Accepted 29 March 2019

Editor: Christine Foyer, Leeds University, UK

Abstract

Nitrate and ammonia deferentially modulate primary metabolism during the hypersensitive response in tobacco. In this study, tobacco RNAi lines with low nitrite reductase (NiR^r) levels were used to investigate the roles of nitrite and nitric oxide (NO) in this process. The lines accumulate NO_2^-, with increased NO generation, but allow sufficient reduction to NH_4^+ to maintain plant viability. For wild-type (WT) and NiR^r plants grown with NO_3^-, inoculation with the non-host biotrophic pathogen *Pseudomonas syringae* pv. *phaseolicola* induced an accumulation of nitrite and NO, together with a hypersensitive response (HR) that resulted in decreased bacterial growth, increased electrolyte leakage, and enhanced pathogen resistance gene expression. These responses were greater with increases in NO or NO_2^- levels in NiR^r plants than in the WT under NO_3^- nutrition. In contrast, WT and NiR^r plants grown with NH_4^+ exhibited compromised resistance. A metabolomic analysis detected 141 metabolites whose abundance was differentially changed as a result of exposure to the pathogen and in response to accumulation of NO or NO_2^-. Of these, 13 were involved in primary metabolism and most were linked to amino acid and energy metabolism. HR-associated changes in metabolism that are often linked with primary nitrate assimilation may therefore be influenced by nitrite and NO production.

Keywords: Amino acid metabolism, nitrate, nitric oxide, nitrite, nitrite reductase.

Introduction

Nitric oxide (NO) has well-established roles in plant physiology and metabolism (Mur *et al.*, 2013a). Key early reports focused on the role of NO in contributing to the hypersensitive response (HR) form of pathogen-elicited programmed

cell death (Delledonne *et al.*, 1998; Durner *et al.*, 1998). Subsequent work has placed NO as playing an integral role the network of host–pathogen elicitory events that govern the outcome of this interaction. NO is not only involved in HR as a part of effector-triggered immunity (ETI) (Delledonne *et al.*, 1998) but it is also induced by pathogen-associated molecular patterns (PAMPs) (Zeidler *et al.*, 2004), and it is involved in controlling the formation of cell-wall appostions (papillae) in host resistance to penetration (Prats *et al.*, 2005). With regards to mechanisms of NO generation in plants, the importance of nitrate reductase (NR) functioning as a nitrite reductase is now well established (Gupta *et al.*, 2011). This places NO generation within the context of a series of reactions including NAD(P)H-dependent NO_3^- reduction to NO_2^- by NR, and subsequently via nitrite reductase (NiR) through to NH_4^+. An alternative step mediated by NR diverts the nitrogen (N) flow towards NO and away from NH_4^+ ($NO_3^- \rightarrow NO_2^- \rightarrow NO^+$).

NO is not the only signalling molecule within the N economy in plants. NO_3 signaling can potentiate its own assimilation through the induction of high- and low-affinity nitrate transporters. It also induces the expression of genes involved in bioenergy, particularly the linked pentose phosphate and glycolytic pathways (Wang *et al.*, 2000). More recent transcriptome studies have examined NO_3^--mediated glutaredoxin expression and implicated this N form in the maintenance of cellular redox homeostasis (Patterson *et al.*, 2016). Many NO_3^- signaling components have now been defined including a series of transcription factors, with NODULE INCEPTION-LIKE PROTEIN7 (NLP7) arguably being one of the most important signalling proteins (Castaings *et al.*, 2009). Another key regulatory component is NITRATE REGULATORY GENE2 (NRG2), which interacts with NLP7 and regulates the expression of the key nitrate transporter *NRT1.1* (Xu *et al.*, 2016). Reports have also suggested that the major N assimilate glutamate could influence the expression of stress-responsive genes (Kan *et al.*, 2015).

Unlike NO_3^-, the discrete signalling roles of NO_2^- in the plant N economy have not been extensively examined. Kasten *et al.* (2016) demonstrated that fumigation of Arabidopsis plants with >20 ppm of NO_2 gas caused cell death. They found increased *S*-nitrosylation and tyrosine nitration, and a protective role of salicylic acid against NO_2^--induced cell death. However, this fumigation approach has drawbacks in defining the effects of NO_2^-, which it can be oxidised to NO_3^-. Previously, Wang *et al.*, (2007) used Arabidopsis Col-0 and a NR-null mutant to unequivocally demonstrate gene expression patterns that were responsive to NO_2^- but not to NO_3^-. An alternative approach has been to examine the phenotypes of NiR-deficient plants, which display high levels of NO_2^-. NiR-deficient tobacco plants have been reported to be chlorotic, under-developed, and to contain reduced protein contents, even when they are supplied with N as NH_4^+ (Vaucheret *et al.*, 1992).

Our previous work focused on NO_3^- or NH_4^+ nutrition during HR elicited by *Pseudonomonas syringae* pv. *phaseolicola* (Psph) in tobacco plants (Gupta *et al.*, 2013). However, this could only correlate NO_3^- effects with NO and was not able to consider the possible contribution of NO_2^-. The latter is particularly relevant as it is known to accumulate during cell death as elicited by cryptogein, a proteinaceous elicitor from *Phytophthora cryptogea* (Planchet *et al.*, 2006). In this current study, we exploit the well-characterised tobacco nitrite reductase-suppressed line 271 (hereafter designated as line NiR^r) (Morot-Gaudry-Talarmain *et al.*, 2002) under NO_3^- or NH_4^+ nutrition regimes. Using NiR^r allowed us to target NO_2^-/NO effects following challenge with Psph. These effects were shown to particularly impact on patterns of amino acid biosynthesis and bioenergetic pathways that have previously been linked to NO_3^- effects. We propose that the NiR^r line reveals previously hidden regulatory events in N flux during plant responses to pathogens.

Material and methods

Plant material

Seeds of tobacco (*Nicotiana tabacum*) cv. Gatersleben (wild-type, WT) were germinated on vermiculite under a 14/10 h day/night regime at 24/20 °C, a relative humidity of 80%, and 350–400 μE^{-2} s^{-1} photosynthetically active radiation (PAR). This study also included the Gatersleben transgenic RNAi transgenic line 271 (NiR^r), which is deficient in NiR (Morot-Gaudry-Talarmain *et al.*, 2002). After 3 weeks, the plants were transferred to hydroponic culture for an additional 5 weeks. Plastic pots, each containing 1.8 l nutrient solution, were kept in a growth chamber with artificial illumination (HQI 400W; Schreder, Winterbach, Germany) at a PAR of 300 µmol m^{-2} s^{-1} with 16-h daily light periods. The day/night temperature regime of the chamber was 24/20 °C. The NO_3^- nutrient solution (pH 6.3) contained 3 mM KNO_3, 1 mM $CaCl_2$, 1 mM $MgSO_4$, 0.025 mM NaFe-EDTA, 0.5 mM K_2HPO_4, 1 mM KH_2PO_4, and trace elements. The NH_4^+ nutrient solution (pH 6) contained 3 mM NH_4Cl, 1 mM $CaCl_2$, 2 mM $MgSO_4$, 25 µM NaFe-EDTA, 0.5 mM K_2HPO_4, 1 mM KH_2PO_4, and trace elements. The nutrient solutions were changed three times a week.

Growth of plant pathogen and inoculation

Pseudomonas syringae pv. *phaseolicola* strain Psph 1448A was grown at 28 °C in King's B medium containing the appropriate antibiotics (Zeier *et al.*, 2004). Overnight log-phase cultures were washed three times with 10 mM $MgCl_2$ and diluted to a final concentration of 10^5 cells ml^{-1}. The bacterial suspensions were infiltrated from the abaxial side into leaves using a 1 ml syringe without a needle. Control inoculations were performed with 10 mM $MgCl_2$ alone. The inoculations were performed when plants had been growing in the nutrient solutions for 4 weeks, and in each case a fully mature leaf was inoculated. *In planta* bacterial growth was assessed using disks taken from the infiltrated areas of three leaves from different plants at 24 h after inoculation. The leaf disks were homogenised in 1 ml of 10 mM $MgCl_2$, plating appropriate dilutions on King's B medium, and counting colony numbers after incubating the plates at 28 °C for 2 d. Comparable samples were also taken from control plants.

Estimation of electrolyte leakage

Loss of membrane integrity was estimated by electrolyte leakage in 1-cm diameter leaf disks taken from the inoculated areas of leaves from three different plants as described by Mur *et al.* (1997). Kinetics of cell death were determined by this method.

Measurement of nitrite content

Leaf disks (1-cm diameter) were taken from three different inoculated and uninoculated plants. Each sample (100 mg) was extracted in 1 ml buffer that contained 50 mM HEPES, pH 7.2, and 100 μM $MgCl_2$, and 100 μl of extract was added to a reaction mixture containing: 600 μl sulfanilamide (1%), 600 μl *N*-(1)-(Naphthyl)ethylene-diaminedihydrochloride (0.02%), and 125 μl zinc acetate (0.5 mM). After incubation for 25 min at 24 °C the samples were centrifuged at 16 000 *g* for 5 min, and the NO_3^- content of the supernatant was determined spectrophotometrically (Hageman *et al.*, 1980).

RNA extraction and gel blot hybridisation analysis

Leaf samples were harvested after infiltration of leaves with Psph or with the control, the infiltrated areas with $MgCl_2$. Total RNA was extracted with PEQ Gold RNAPure® reagent (PEQ LAB, Erlangen, Germany) according to the manufacturer's instructions. The RNA obtained was separated on 1.5% agarose gels containing 5.5% formaldehyde, and blotted into nylon membranes. The nucleic acids bound to the membrane were cross-linked by UV-irradiation for 2 min. The expression of *Pathogenesis related protein 1* (*PR1*) provides a marker for NO-elicited production of the defence hormone salicylic acid (Mur *et al.*, 2000, 2013b). *PR1* probes were labelled to high specific activity using the Random Primer DNA labelling system with 40 μCi [α-^{32}P] dCTP (ICN Biomedicals, Eschwege, Germany) according to the supplier's instructions. Hybridisation was performed at 65 °C for 15 h in 1% BSA, 1 mM EDTA, and 0.5 M Na_2HPO_4. The membrane was washed with 2× saline sodium citrate (SSC), 0.1% SDS at 65 °C for 30 min, and afterwards with 0.2× SSC, 0.1% SDS for 15 min at 65 °C prior to autoradiography. The air-dried membrane was exposed to Kodak X-omat DS film (Stuttgart, Germany) with an intensifying screen at −80 °C and the film was developed after appropriate time intervals.

NO measurement using a quantum cascade laser

The use of a quantum cascade laser (QCL) to detect NO has been described previously (Mur *et al.*, 2011). The system allows on-line NO measurements with a detection limit of 0.8 ppbv in 1 s (Mandon *et al.*, 2016). Detached tobacco leaves were placed in a glass cuvette (200 ml volume) with an air inlet and outlet, and NO production was monitored at a controlled continuous flow rate of 1 l h^{-1}. Multiple cuvettes could be monitored in sequence, each being measured for ~13 min. The laser light emitted by the QCL (at ~1850 cm^{-1}) passed through a multi-pass absorption cell where the NO molecules are transported via the airline. The intensity of the transmitted laser light is strongly attenuated due to NO absorption in the multi-pass cell (effective path length=76 m), following the Beer–Lambert law. The detected signal depends of the laser intensity before the multi-pass cell, the absorption length, and the absorption coefficient of NO at the given wavelength. The NO concentration was calculated by measuring the attenuation of the light coming into the cell relative to the transmitted light (after the cell). Following measurement, the fresh weight of the leaves inside the cuvettes was determined.

Metabolite profiling

Gas chromatograph–mass spectrometry (GC-MS) analysis was performed as described previously (Cuadros-Inostroza *et al.*, 2009). Six replicates each consisting of six pooled plants obtained from two independent experiments were subjected to GC-MS analysis. Metabolite levels were determined in a targeted fashion using the TargetSearch software (Cuadros-Inostroza *et al.*, 2009). Metabolites were selected by comparing their retention indexes (+/− 2 s) and spectra (similarity >85%) against the compounds stored in the Golm-Metabolome-Database (GMD) (Kopka *et al.*, 2005), resulting in the identification of 141 metabolites. Each metabolite is represented by the observed ion intensity of a selected unique ion, which allows for a relative quantification between groups. Metabolite data were log_{10}-transformed. In addition, total amino acids were measured by HPLC described previously by Mahmood *et al.* (2002). Data were subjected to ANOVA using Minitab v.14. Comparisons between treatments were performed using Tukey multiple pairwise comparisons. Time-course data were compared using ANOVA. Principal component analyses and hierarchical cluster analyses were performed using the MetaboAnalyst software (Xia *et al.*, 2015).

Results

Effects of N source on NO_2^-, NH_4^+, total amino acids, and NO production

Wild-type (WT) and NiR^r tobacco plants (n=6 per genotype) were grown hydroponically and supplied with NO_3^- or NH_4^+ nutrient solutions for a 5-week period, after which leaves were sampled. At this stage the leaves were viable and apparently fully green, although in line with a previous report the NiR^r plants were smaller (Morot-Gaudry-Talarmain *et al.*, 2002). In plants fed with NO_3^- there was a substantial and significant accumulation of NO_2^- (>5-fold compared to the WT) due to lower rates of reduction to NH_4^+ (Fig. 1A). When fed with NH_4^+, WT plants exhibited negligible levels of NO_2^- as the NR-dependent N assimilation pathway was circumvented. The NH_4^+ content in plants fed with NH_4^+ did not significantly differ between the WT and NiR^r (Fig. 1B). The lower amounts of NH_4^+ in WT plants fed with NO_3^- presumably reflected the effects of N assimilation. The total amino acid contents of WT and NiR^r plants significantly differed according to the type of N nutrition (Fig. 1C). We next assessed NO production using a QCL-based system and the results indicated

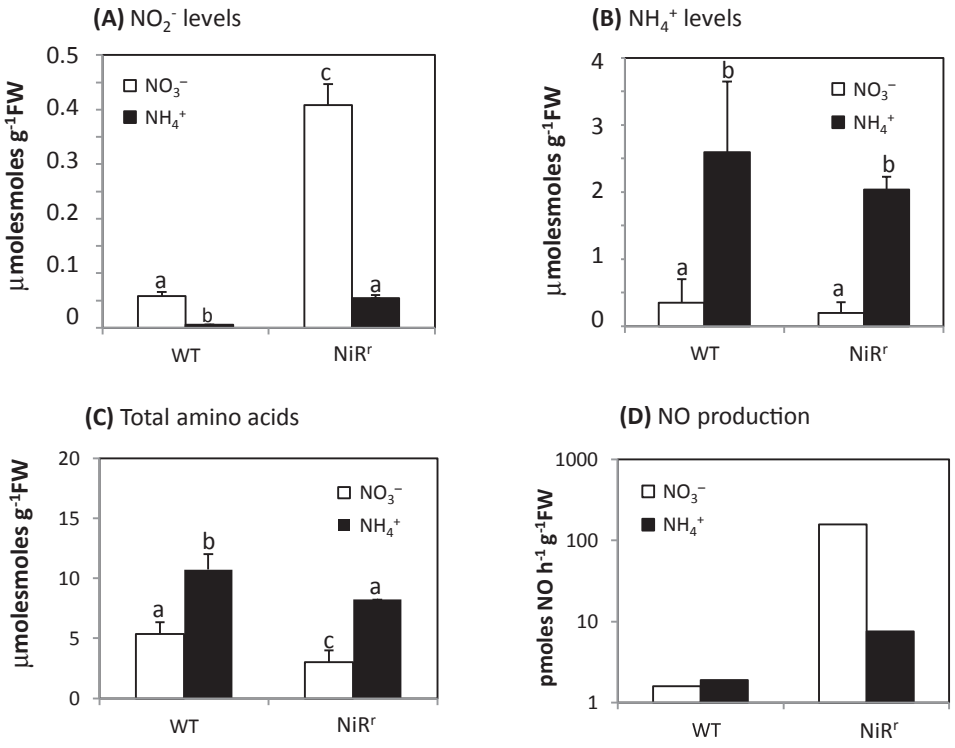

Fig. 1. Impact of suppression of nitrite reductase on transgenic tobacco. Comparisons of the wild-type (WT) and the RNAi line 271 suppressed in nitrite reductase (NiR^r) following hydroponic feeding with either NO_3^- or NH_4^+ nutrient solutions. Accumulation of (A) NO_2^-, (B) NH_4, and (C) total amino acid. (D) Nitric oxide production as determined using a quantum cascade laser-based system. All measurements were taken on leaves of plants at 6 weeks old. Data are means (±SE) of n=3 replicate plants. Different letters indicate significant differences between means as determined using ANOVA (P<0.05).

negligible production in WT and NiR^r plants fed with NH_4^+ (Fig. 1D; note the log scale). However, feeding NO_3^- to NiR^r resulted in >100-fold increase in NO production compared to the equivalent WT plants.

Effects of N source on the hypersensitive response to a non-host pathogen

Leaves of WT and NiR^r plants fed with either NH_4^+ or NO_3^- were inoculated with the non-host pathogen *P. syringae* pv *phaseolicola* (Psph), or with a control solution of 10 mM $MgCl_2$ and the resulting phenotypes were assessed after 24 h. No symptoms were seen in control WT or NiR plants (Fig. 2A) but some signs of HR-associated necrosis were observed in WT plants fed with NO_3^-following inoculation with Psph. Necrotic symptoms were much more evident in leaves of NiR^r plants fed with NO_3^- (Fig. 2B). In line with HR-elicited NO production being dependent on the reduction of NO_3^- and NO_2^- (Gupta *et al.*, 2011), in the WT only plants fed with NO_3^-exhibited increased NO levels (Fig. 2C). The increase in NO production was substantially greater in NiR^r plants. Some increased NO production was found in NiR^r plants fed with NH_4^+, which probably reflects the residual NO_3^- concentrations observed in this genotype (Fig. 1).

The patterns of NO generation were broadly in line with other observed defence parameters. We assessed electrolyte leakage as a quantitative measure of cellular stress and death, and the most rapid increase was observed NiR^r plants fed with NO_3^- (Fig. 3A). Increases in electrolyte leakage were also seen in the other treatments, but there was a notably slower and lower response in WT plants fed with NH_4^+. This was consistent with some increased stress that might be linked to the ultimate formation of a HR (Gupta *et al.*, 2013). The delayed deployment of defences in WT plants fed with NH_4^+ - was associated with increased numbers of Psph bacteria compared to plants fed with NO_3^- (Fig. 3B). A similar pattern was observed in NiR^r plants but it was not so pronounced, presumably due to the effects of NO production in this genotype (Fig. 2C). The expression of *PR1* provides a marker for NO-elicited production of the defence hormone salicylic acid, and significant induction was only seen following feeding with $NO_3^-$and was much more pronounced in NiR^r plants in comparison to the WT (Fig. 3C).

Effects of N source on the metabolomic impact of a non-host pathogen

Principal component analysis (PCA) was initially employed to describe the effects of the N regimes on the plant responses to inoculation with Psph. This revealed that challenge with Psph had relatively minor impacts on the metabolomes with respect to background genotypic effects (Fig. 4A). However, to better visualise the effects, each genotype was considered in isolation and this indicated that the greatest Psph-elicited effects were seen in NiR^r plants at 24 h post inoculation (hpi) but at 12 hpi in the WT (Fig. 4B, C).

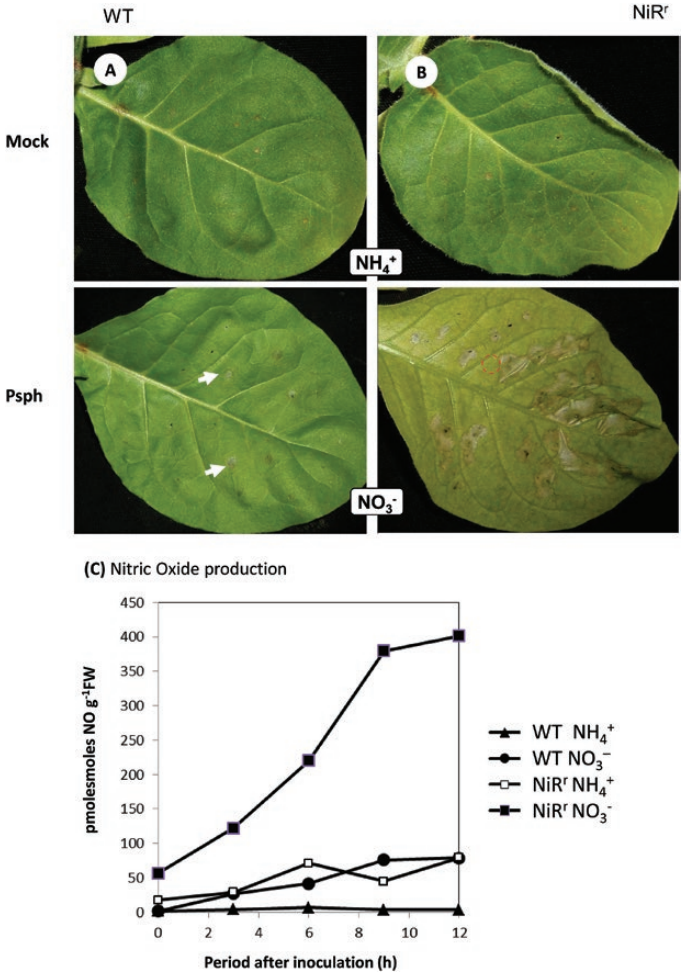

Fig. 2. Phenotypic responses and NO production in wild-type (WT) and transgenic tobacco plants with suppression of nitrite reductase (NiR^r) following inoculation with *Pseudomonas syringae* pv *phaseolicola* (Psph) in 10 mM $MgCl_2$. Plants were subject to hydroponic growth with either NO_3^- or NH_4^+ nutrient solutions prior to inoculation. Lesion development at 24 h after inoculation in leaves of (A) the WT and (B) NiR^r plants. Plants in the mock control were inoculated with 10 mM $MgCl_2$ only. Symptoms were more frequent and severe in NiR^r plants than in the WT when grown with NO_3^-. The hypersensitive response was strongly delayed in plants grown with NH_4^+. Arrows indicate small lesions in the WT. The images are representative of five independent experiments. (C) Nitric oxide production as determined using a quantum cascade laser-based system in WT and NiR^r plants following inoculation with Psph. Representative data from one of three biological replicates are shown.

We next examined metabolites known to be associated with plant defence, namely linolenic acid (a jasmonate precursor), salicylic acid, dehydroascorbate and α-tocopherols (both indicators of oxidative status), and the polyamines putrescine, GABA, and spermidine (Fig. 5). As expected, linolenic and salicylic acid both exhibited initial increases in WT plants following Psph inoculation. In NiR^r plants, the Psph-elicited synthesis of linolenic acid was dramatically increased; in contrast, levels of salicylic acid were already elevated and did not exhibit any further significant increase following infection. Dehydroascorbate, the oxidised form of ascorbate, was also elevated in NiR^r plants prior to infection, most notably for plants fed with NO_3^-, suggesting that the plants were under oxidative stress prior to pathogen challenge. This increased stress did not appear to be reflected in the levels of α -tocopherol, a lipophilic antioxidant. The levels of linolenic acid, salicylic acid, and dehydroascorbate were all elevated in NiR^r plants post inoculation when fed with either N form, and these are likely to be NO_2^-/NO effects. Different patterns were seen for polyamine metabolism, where feeding with NH_4^+ appeared to increase the amount of GABA in NiRr-NH_4^+, but there was a dramatic increase in NiR^r-NO_3^- at 24 hpi whilst feeding with NO_3^- elevated spermidine levels in NiR^r plants at all time points. Feeding with NO_3^- also caused increase in spermidine levels in WT plants. Thus, NH_4^+ and NO_2^-/NO are likely to be influencing different steps in polyamine metabolism.

We next schematically plotted the combined effects of imposing biotic stress, suppression of NiR, and differential N feeding in order to highlight their impact on amino acid metabolism and as a means of identifying possible co-regulatory routes (Fig. 6). Elicitation of HR led to a variety of amino acid responses. Those using phosphoenolpyrruvate (PEP) for their carbon skeleton were markedly reduced in NiR^r plants fed with NO_3^-, although phenylalanine levels were broadly maintained or increased following Psph inoculation. This may reflect prioritisation for phenylalanine biosynthesis to feed defence-associated biosynthesis of phenylpropanoids and flavonoids. For pyruvate and TCA-derived metabolites, each was increased or, in the case of α-ketoglutarate, maintained in response to Psph in NiR^r plants. Of the pyruvate-derived amino acids, there was an increase in alanine on infection at 12 hpi under both feeding regimes in NiR^r plants, was although levels declined with NH_4^+ at 24 hpi. Levels of valine in NiR^r plants showed no increase associated with Psph and declined in plants fed NO_3^-. The α-ketoglutarate derivatives glutamate and glutamine did not vary significantly in the NiR^r plants whilst proline levels increased in plants fed with NH_4^+ to match those seen following feeding with NO_3^-.

The oxaloacetate route demonstrated the greatest variety of responses. Asparate and methionine transiently increased in NiR^r plants fed with either N form at 12 hpi. In the case of asparagine, this transient increase was only seen in - NiR^r plants fed with NO_3^-. For lysine, a similar increase at 12 hpi was also observed but only in the WT lines, irrespective of the N-feeding regime. Threonine gave the most distinct pattern with NiR^r plants fed with NH_4^+ showing increases following inoculation with Psph.

Other aspects of primary metabolism were visualised using a heat map (Fig. 7). This indicated two classes of response, namely metabolites that were induced in NiR^r plants or those that were induced in WT plants. Most metabolites showed only marginal changes following challenge with Psph. As with uninfected plants, glyceraldehyde-3-phosphate, fumarate, and malate appeared to be elevated whenever NO production was increased, suggesting a coordinated response between amino acid biosynthesis and the bioenergetic pathways in response to alterations in N nutrition.

Discussion

NiR transgenic lines facilitate analyses of the effects of N forms on plant physiology

Far from only acting as components in the nitrogen assimilation pathway, NO_3^- and NO_2^- (and possibly NH_4^+)

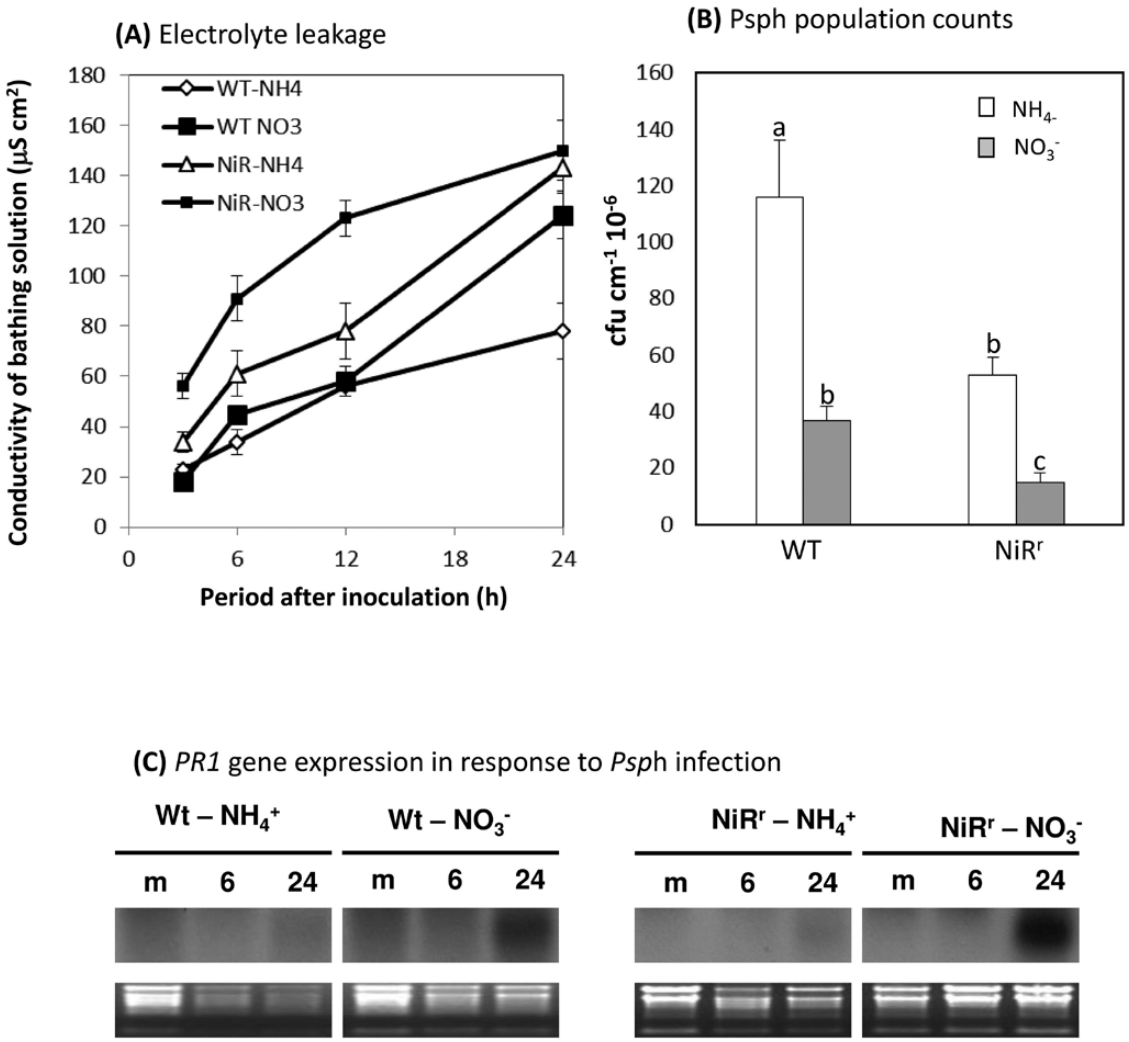

Fig. 3. Effects of inoculation with *Pseudomonas syringae* pv *phaseolicola* (Psph) on wild-type (WT) and transgenic tobacco plants with suppression of nitrite reductase (NiR^r). Plants were subject to hydroponic growth with either NO_3^- or NH_4^+ nutrient solutions prior to inoculation. (A) Electrolyte leakage in leaves 0–24 h after inoculation. (B) Bacterial growth on leaves measured at 24 h after inoculation. Data are means (±SE) of n=6 replicates. Different letters indicate significant differences between means as determined using ANOVA (P<0.05).(C) *PR1* gene expression in response to Psph infection. Representative data from one of three biological replicates are shown.

are emerging alongside NO as signalling components that influence important facets of primary metabolism. NO_3^- signaling events have already been well characterised at the molecular level (Castaings *et al.*, 2009; Xu *et al.*, 2016). Whilst studies on NO_2^- are not so advanced, transcriptomic experiments have established some overlapping effects of NO_3^- and NO_2^- on gene expression in Arabidopsis (Wang *et al.*, 2007). NH_4^+ has been considered to be toxic at high levels and the bacterial tabtoxin produced by *P. syringae* pv. *tabaci* inhibits glutamine synthetase in plants, elevating NH_4^+ and initiating chlorosis (Langston-Unkefer *et al.*, 1987). However, we have previously found that feeding with NH_4^+ can also bias N metabolism towards the production of GABA (Gupta *et al.*, 2013), a nutrient source for some pathogens (Solomon and Oliver, 2001; Borrero *et al.*, 2012). In contrast, feeding plants with NO_3^- shifts metabolism towards increased resistance that correlates with elevated NO and polyamine production (Gupta *et al.*, 2013). Crucially, these effects could reflect contributions from NO_3^-/NO or NO_2^-/NO, or a combination of all three N forms. Our current study aimed to address the question as to the relative involvement of these forms of nitrogen.

The difficulty in investigating the roles of any particular N form lies in their facile reduction, or in some cases oxidation, to other forms. Thus, although Kasten *et al.* (2016) treated plants with NO_2 gas, this resulted in the generation of variety of N forms. Wang *et al.*, (2004) addressed this problem by generating NR null mutants, which could not reduce NO_3^- to NO_2^-. In this current work, we exploited a previously characterised transgenic line that is suppressed in NiR (NIR^r), which would allow NO_2^- accumulation relative to WT lines. Our initial assessment of the accumulation of different forms of N in NiR^r plants were in line with the previous observations of Morot-Gaudry-Talarmain *et al.*, (2002). Thus, the NiR^r plants are able to highlight any NO_2^-/NO-mediated effects that were hidden in our previous analyses based on feeding of WT tobacco with NO_3^- (Gupta *et al.*, 2013). However, our approach had some difficulties as NO would also accumulate in NIR^r plants fed

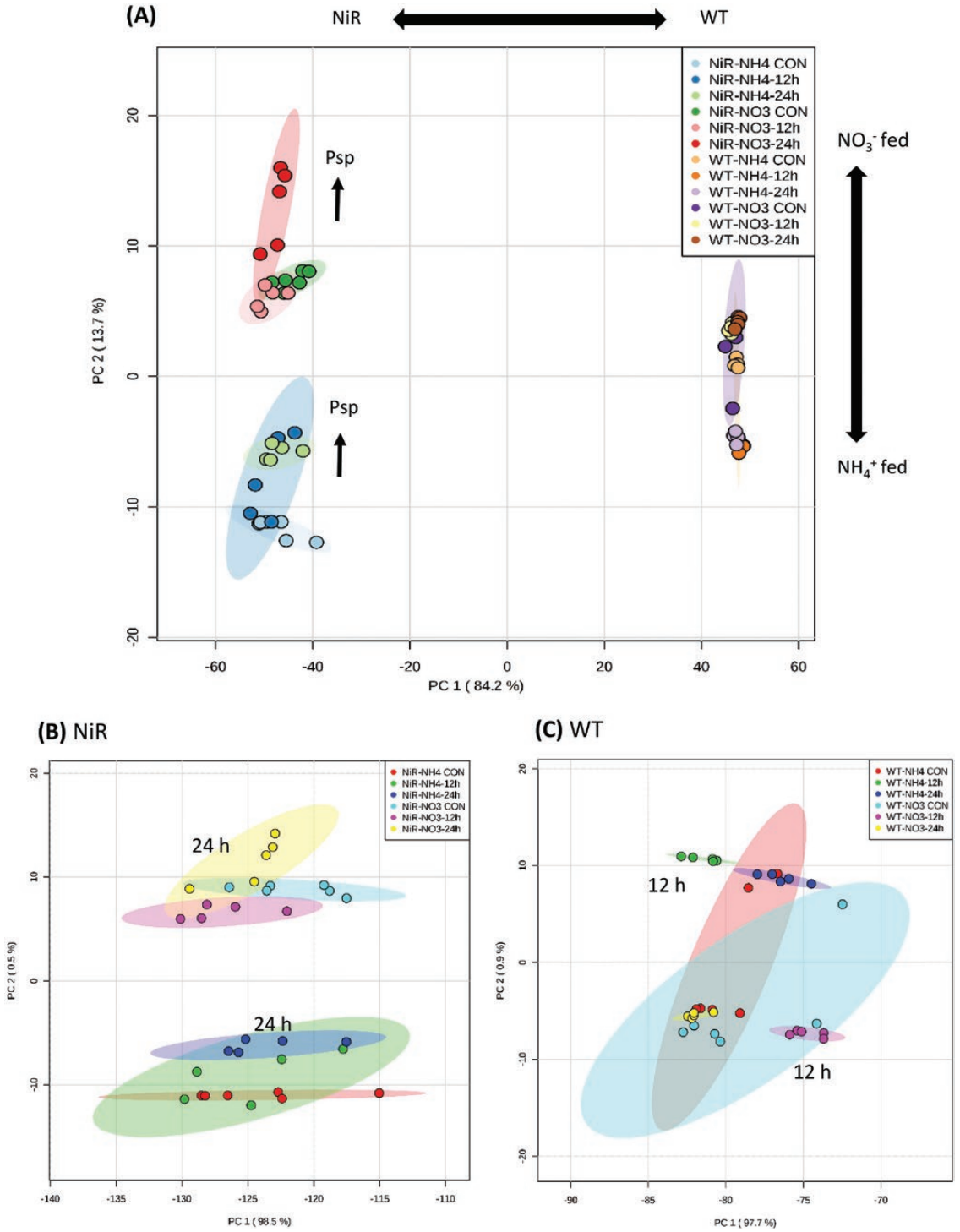

Fig. 4. Metabolomic assessment of the impact of *Pseudomonas syringae* pv. *phaseolicola* (Psp) inoculation on wild-type (WT) and transgenic tobacco plants with suppression of nitrite reductase (NiR^r). Plants were subject to hydroponic feeding with either NO_3^- or NH_4^+ nutrient solutions prior to inoculation. Samples for analysis were taken from leaves at 12 h and 24 h after inoculation and also from control mock inoculated leaves (n=6 replicates). (A) Principal component analysis (PCA) of 141 metabolites as detected by gas chromatography–mass spectrometry. (B, C) Sub-analysis of the same dataset focusing only on the responses of (B) NiR^r and (C) WT plants. The shaded areas indicate 95% confidence intervals for each experimental class.

with NO_3^-, so we could not dissect NO_2^- from NO effects. NiR^r plants fed with NH_4^+ could indicate effects of this particular form of N, but we did note some very minor accumulation of NO_2^- (Fig. 1A) and some minimal generation of NO (Fig. 1D). This NO_2^- accumulation could reflect contributions of N from plant-associated microbes. Interestingly, low levels of NH_4^+ were detected in NiR^r plants even with NO_3^-,most likely arising from residual activity of NiR (Fig 1C). This low level of NH_4^+ seemed to be able to maintain the viability of NiR^r plants when feeding with NO_3^-.

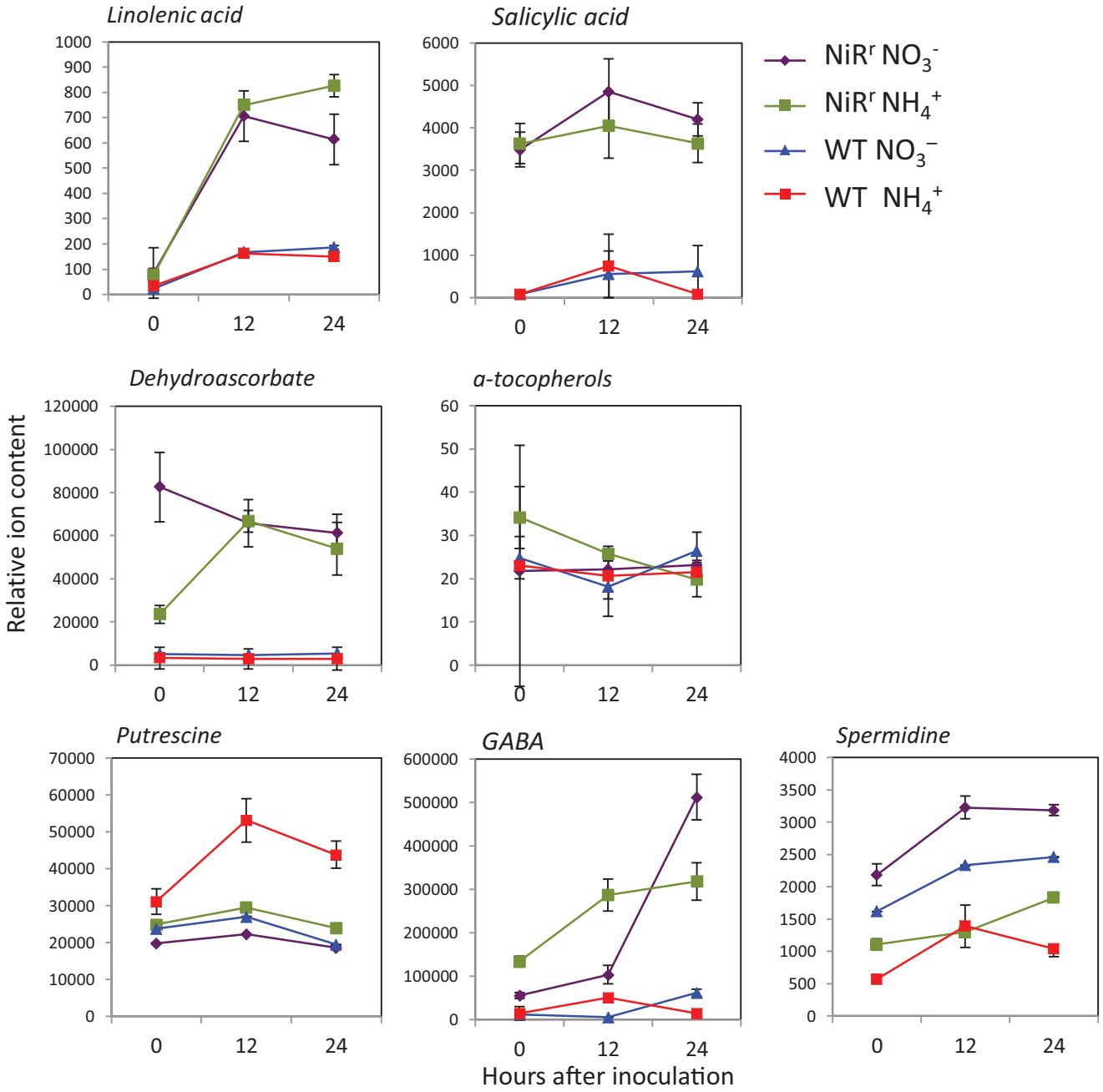

Fig. 5. Changes in defence-associated metabolites in response to *Pseudomonas syringae* pv. *phaseolicola* inoculation on wild-type (WT) and transgenic tobacco plants with suppression of nitrite reductase (NiR^r). Plants were subject to hydroponic feeding with either NO_3^- or NH_4^+ nutrient solutions prior to inoculation. Samples for analysis were taken from leaves at 0, 12h24 h after inoculation (n=6 replicates). Data show means (±SE) of relative accumulation of metabolites (see Methods).

Discrete roles for NO_2^-/NO and NH_4^+ during a non-host HR in tobacco

The results obtained from the NiR^r line could potentially be artefacts, and therefore we aimed to concentrate on situations where NH_4^+ and NO_2^- would be accumulating in WT plants so that their specific effects could be examined. NH_4^+ accumulation is considered to be toxic and there appear to be no non-pathological situations under which it accumulates. Exogenous application has been shown to confer resistance against *P. syringae* in tomato, most likely through the initiation of oxidative stress to confer resistance (Fernandez-Crespo *et al.*, 2015). By contrast, we have previously found that NH_4^+ contributes to susceptibility to *P. syringae* in tobacco, possibly by diverting metabolism towards GABA as an N nutrition source (Gupta *et al.*, 2013). The concentration of applied NH_4^+ was similar in our study to that of Fernández-Crespo *et al.*, (2015) except that we used NH_4Cl instead of $(NH_4)_2SO_4$. There are well-established situations where NO_2^- can accumulate, especially where substantial NO production is required during a HR (Gupta *et al.*, 2011). The HR is therefore a situation where both NO and NO_2^-could have discrete effects from other NO forms. Kasten *et al.*, (2016) also found the NO_2^- could

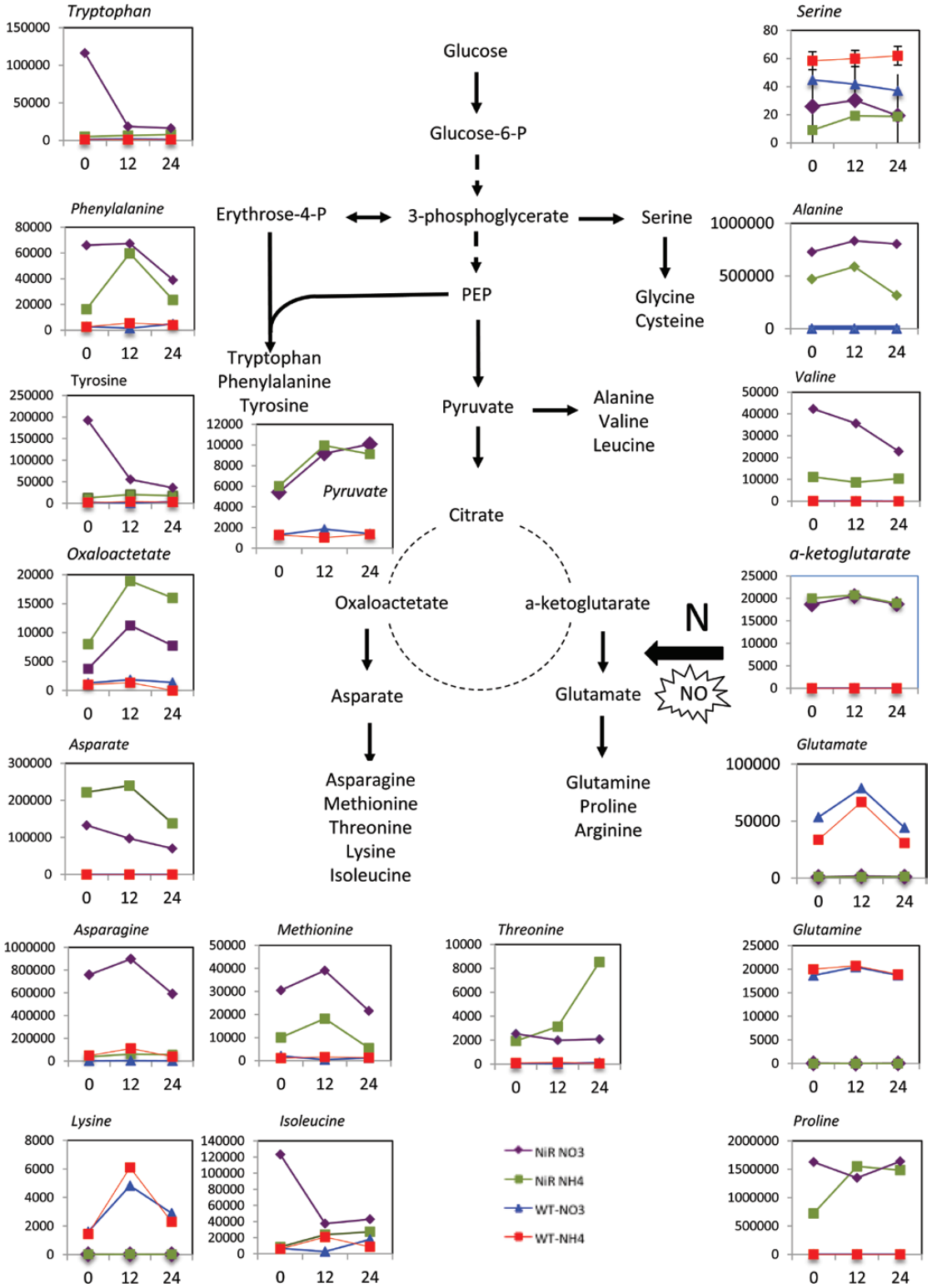

Fig. 6. Changes in amino acid accumulation in response to *Pseudomonas syringae* pv. *phaseolicola* inoculation on wild-type (WT) and transgenic tobacco plants with suppression of nitrite reductase (NiR^r). Plants were subject to hydroponic feeding with either NO_3^- or NH_4^+ nutrient solutions prior to inoculation. Samples for analysis were taken from leaves at 0–24 h after inoculation (n=6 replicates). Data show means (±SE) of relative accumulation of amino acids and providers of amino-acid carbon skeletons. are plotted against the schematic diagram used in Fig. 6

be linked to programmed cell death. Thus, our approach based on NiR^r plants allowed us to assess how far NO_2^-/NO could be influencing the HR as opposed to NO_3^-/NH_4^+. Furthermore, the challenge with Psph would produce a stress situation in which amino acid catabolism could predominate over anabolism (Less and Galili, 2009).

Assessments of broad parameters linked to the HR confirmed the influence of NO/NO_2^- effects on the kinetics of

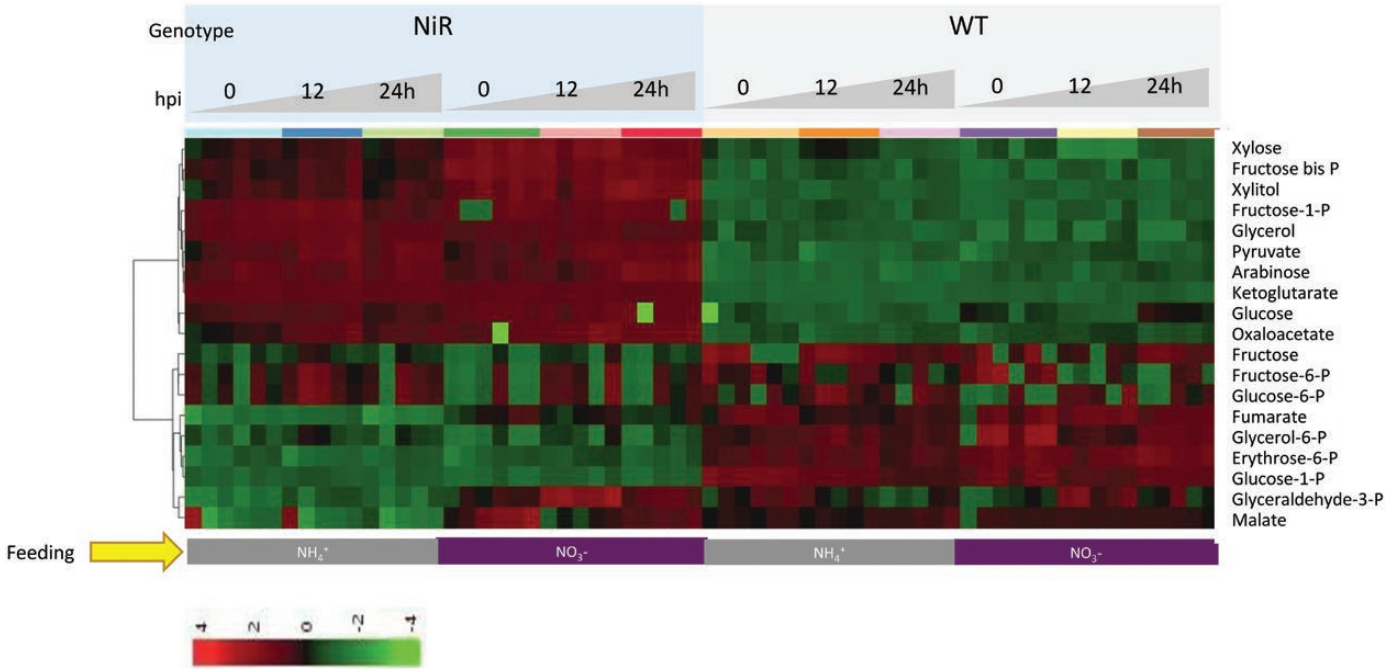

Fig. 7. Impact on bioenergetic-associated metabolites in response to *Pseudomonas syringae* pv. *phaseolicola* inoculation on wild-type (WT) and transgenic tobacco plants with suppression of nitrite reductase (NiR^r). Plants were subject to hydroponic feeding with either NO_3^- or NH_4^+ nutrient solutions prior to inoculation. Samples for analysis were taken from leaves 0, 12h,24 h post inoculation (hpi; *n*=6 replicates). Hierarchical cluster analysis was performed on data acquired by gas chromatography–mass spectrometry and a heat map was constructed for metabolites associated with the pentose phosphate, glycolysis, and TCA cycles.

cell death, resistance to Psph, and *PR1* expression as a biomarker for salicylic acid accumulation (Fig. 3). These are all well established as being linked to NO-mediated events (Delledonne *et al.*, 1998). We chose to focus on the impact of N form on the metabolome in order to align with our previous study (Gupta *et al.*, 2013; Mur *et al.*, 2017). Wang *et al.* (2004, 2007) used a transcriptomic approach to demonstrate that nitrite at micromolar concentrations is able to induce changes in expression linked to primary metabolism, especially bioenergetic pathways and amino acid biosynthesis. As such pathways are also under allosteric control that would not be reflected in gene expression profiles, in our current study we adopted a metabolomic approach in order to reveal actual changes in key metabolites (as also suggested by Kusano *et al.*, 2011) and thus to improve our understanding of nitrogen metabolism.

Our current study clearly indicated that our previous observed effects on GABA and spermidine (Gupta *et al.*, 2013) were linked to NO_2^-/NO effects rather than to NO_3^-. Increases in putrescine were again linked to NH_4^+ application (Fig. 1B, Fig. 5) and seemed not to be linked to any antioxidant/stress hormone effect (Fig. 5). Further work is needed to establish the mechanistic basis of such NH_4^+ effects. More broadly, and in line with the studies of Wang *et al.* (2004, 2007), our metabolomic approach showed that major sources of variation between plants fed with the different forms of N were in metabolites associated with bioenergetic pathways (glycolysis, TCA cycle, and pentose phosphate pathways) and linked to amino acid biosynthesis (Supplementary Table S1 at *JXB* online). Many studies have linked the HR to metabolic pathways that drive increased carbon flux through the TCA cycle, and this has been presumed to serve the energetic demands of defence, and to be linked to the HR form of programmed cell death (Bolton *et al.*, 2009); Balmer *et al.*, 2018). Our data from NiR^r plants would suggest that these effects on primary metabolism are influenced by NO_2^-/NO. Indeed, several of the steps previously linked to NO_3^-, particularly in the pentose phosphate and glycolytic pathways (Wang *et al.*, 2000) , appeared to be influenced by NO_2^-/NO in our study.

Given the obvious links with N assimilation and NO, much of our analyses focused on amino acid accumulation (Galili *et al.*, 2016). A series of bioinformatic analyses have indicated that genes involved in amino acid catalysis are the most responsive to stress conditions (Less and Galili, 2008, 2009). Complementary to this, Less and Galili (2009) identified a 'Met metabolism module' with the asparate family network being the most active during growth. Beyond differential gene expression, several amino acid enzymes are subject to allosteric regulation, often by the end-products of various branches of the amino acid biosynthetic pathways. Our examination of the differential patterns of amino acid accumulation suggested changes that could be associated with the different bioenergetic pathways acting as the source of the carbon-skeleton precursors (Fig. 6). However, the patterns in changes that we found in amino acid metabolism bore no similarities to the 'metabolism modules' as defined by the transcriptomic analyses of Less and Galili, (2009).

Examination of amino acid metabolism during the interaction with *Psph* indicated a range of responses in the NiR^r line. We separated the amino acids based on their source of carbon skeletons (Fig. 6) and this demonstrated a range of responses to N forms, with increases (pyruvate) or no significant changes (α-ketoglutarate, serine) on infection under both

feeding regimes. In some cases (tryptophan, tyrosine, asparagine, isoleucine, valine) changes were only seen with NiR^r plants fed with NO_3^-, which would reflect regulation by NO_2^-/NO. The accumulation of these amino acids was dramatically reduced with *Psph* infection, and in the case of tryptophan accords with a report that NO can reduce the expression of genes involved tryptophan-dependent auxin biosynthesis (Elhiti *et al.*, 2013). Assuming that NO was exerting such an effect on the transient increases seen following Psph inoculation, asparagine was slightly differentially regulated as NiR^r plants fed with NO_3^- exhibited a transient increase at 12 hpi before showing a reduction. Whether the regulatory mechanisms involve NO suppression of biosynthetic enzyme gene expression and/or increased amino acid catalysis remains to be established.

For oxaloacetate, methionine) there were transient increases in both N-feeding regimes. This was a perplexing observation, perhaps indicating overlapping and general effects of various N forms. Equally, we observed NO_2^-/NO effects in plants fed with NH_4^+ so these could reflect sensitive responses to NO_2^-/NO. We also found that accumulation of oxaloacetate, asparate, and threonine was increased more following inoculation with Psph in NiR^r plants fed with NH_4^+ than in those fed with NO_3^-. This could be the result of interactions between NH_4^+ and NO_2^- accumulation, or of NO-mediated reduction of biosynthetic gene expression/increased catalysis. The picture is further complicated by glutamate and glutamine where NiR^r plants showed no increases, suggesting either increased catalysis or reduced accumulation/accelerated utilisation.

Whilst, our data suggest a role for NO_2^- acting either alone or via NO, they may not reflect a direct role of either on plant metabolism. Thus, changes in NO/NO_2^-in NiR^r plants clearly have impacts on the redox status and, either directly linked to these or in parallel, there is an accumulation of defence signals (Fig. 5). In this context, NO has already been linked to changes in antioxidants and these can lead to accumulation of salicylate (Durner *et al.*, 1998; Begara-Morales *et al.*, 2016). However, this ignores the signaling roles of glutamate (Forde, 2014). Although not fully characterised, exogenous application of glutamate affects root growth and branching (Walch-Liu *et al.*, 2006), causes stomatal closure (Yoshida *et al.*, 2016), and induces genes involved in nitrogen uptake in roots (Kan *et al.*, 2015), and several glutamate-like receptors (Kong *et al.*, 2015; Singh *et al.*, 2016) and signalling modules have been proposed (Forde, 2014). We found that glutamate accumulation (and therefore any linked signalling) only occurred in situations where NO_2^- accumulation was absent (Fig. 6). Thus, elevated NO_2^-/NO could function in an negative-feedback mechanism to suppress potentially excessive N assimilation, as has been suggested by ourselves and others (Mur *et al.*, 2013b; Frungillo *et al.*, 2014).

One question that remains outstanding from our work concerns the potential differential regulatory role of NO versus NO_2^- in influencing metabolism, and this will be addressed in our future work. However, taken together, our observations have provided clear evidence that N forms influence patterns of metabolism, tailoring them to particular situations through the relative levels of NO_3^-, NO_2^-/NO, and NH_4^+. These patterns serve precise bioenergetic needs for particular development or defence requirements.

Supplementary data

Supplementary data are available at *JXB* online.

Table S1. Major sources of variation resulting from differential feeding of WT and NiR^r tobacco plants with NO_3^- or NH_4^+.

Acknowledgements

The authors wish to thank the UKIERI-DST fund and DBT, DST-SERB for partially funding this work. We declare no conflicts of interest in relation to this work.

Author contributions

JGK, LM, WMK, and ARF conceived the ideas described in this paper; AK provided technical support and aided in reviewing and editing the final manuscript; JGK and LM wrote the manuscript and prepared the figures; YB prepared the metabolomic profiles; YB, AK, ARF, and LM analysed the metabolomic profiles; JZ undertook some preliminary bacterial infection experiments; JM, SMC, LM, and FH undertook NO measurements using the Quantum Cascade system.

References

Balmer A, Pastor V, Glauser G, Mauch-Mani B. 2018. Tricarboxylates induce defense priming against bacteria in *Arabidopsis thaliana*. Frontiers in Plant Science **9**, 1221.

Begara-Morales JC, Sánchez-Calvo B, Chaki M, Valderrama R, Mata-Pérez C, Padilla MN, Corpas FJ, Barroso JB. 2016. Antioxidant systems are regulated by nitric oxide-mediated post-translational modifications (NO-PTMs). Frontiers in Plant Science **7**, 152.

Bolton MD. 2009. Primary metabolism and plant defense–fuel for the fire. Molecular Plant-Microbe Interactions **22**, 487–497.

Borrero C, Trillas MI, Delgado A, Avilés M. 2012. Effect of ammonium/nitrate ratio in nutrient solution on control of *Fusarium* wilt of tomato by *Trichoderma asperellum* T34. Plant Pathology **61**, 132–139.

Castaings L, Camargo A, Pocholle D, *et al.* 2009. The nodule inception-like protein 7 modulates nitrate sensing and metabolism in Arabidopsis. The Plant Journal **57**, 426–435.

Cuadros-Inostroza A, Caldana C, Redestig H, Kusano M, Lisec J, Peña-Cortés H, Willmitzer L, Hannah MA. 2009. TargetSearch–a Bioconductor package for the efficient preprocessing of GC-MS metabolite profiling data. BMC Bioinformatics **10**, 428.

Delledonne M, Xia Y, Dixon RA, Lamb C. 1998. Nitric oxide functions as a signal in plant disease resistance. Nature **394**, 585–588.

Durner J, Wendehenne D, Klessig DF. 1998. Defense gene induction in tobacco by nitric oxide, cyclic GMP, and cyclic ADP-ribose. Proceedings of the National Academy of Sciences, USA **95**, 10328–10333.

Elhiti M, Hebelstrup KH, Wang A, Li C, Cui Y, Hill RD, Stasolla C. 2013. Function of type-2 Arabidopsis hemoglobin in the auxin-mediated formation of embryogenic cells during morphogenesis. The Plant Journal **74**, 946–958.

Fernández-Crespo E, Scalschi L, Llorens E, García-Agustín P, Camañes G. 2015. NH_4^+ protects tomato plants against *Pseudomonas syringae* by activation of systemic acquired acclimation. Journal of Experimental Botany **66**, 6777–6790.

Forde BG. 2014. Glutamate signalling in roots. Journal of Experimental Botany **65**, 779–787.

Frungillo L, Skelly MJ, Loake GJ, Spoel SH, Salgado I. 2014. S-nitrosothiols regulate nitric oxide production and storage in plants through the nitrogen assimilation pathway. Nature Communications **5**, 5401.

Galili G, Amir R, Fernie AR. 2016. The regulation of essential amino acid synthesis and accumulation in plants. Annual Review of Plant Biology **67**, 153–178.

Gupta KJ, Brotman Y, Segu S, *et al.* 2013. The form of nitrogen nutrition affects resistance against *Pseudomonas syringae* pv. *phaseolicola* in tobacco. Journal of Experimental Botany **64**, 553–568.

Gupta KJ, Fernie AR, Kaiser WM, van Dongen JT. 2011. On the origins of nitric oxide. Trends in Plant Science **16**, 160–168.

Hageman RH, Reed AJ, Femmer RA, Sherrard JH, Dalling MJ. 1980. Some new aspects of the *in vivo* assay for nitrate reductase in wheat (*Triticum aestivum* L.) leaves. I. Reevaluation of nitrate pool sizes. Plant Physiology **65**, 27–32.

Kan CC, Chung TY, Juo YA, Hsieh MH. 2015. Glutamine rapidly induces the expression of key transcription factor genes involved in nitrogen and stress responses in rice roots. BMC Genomics **16**, 731.

Kasten D, Mithöfer A, Georgii E, Lang H, Durner J, Gaupels F. 2016. Nitrite is the driver, phytohormones are modulators while NO and H_2O_2 act as promoters of NO_2-induced cell death. Journal of Experimental Botany **67**, 6337–6349.

Kong D, Ju C, Parihar A, Kim S, Cho D, Kwak JM. 2015. Arabidopsis glutamate receptor homolog3.5 modulates cytosolic Ca^{2+} level to counteract effect of abscisic acid in seed germination. Plant Physiology **167**, 1630–1642.

Kopka J, Schauer N, Krueger S, *et al.* 2005. GMD@CSB.DB: the Golm Metabolome Database. Bioinformatics **21**, 1635–1638.

Kusano M, Fukushima A, Redestig H, Saito K. 2011. Metabolomic approaches toward understanding nitrogen metabolism in plants. Journal of Experimental Botany **62**, 1439–1453.

Langston-Unkefer PJ, Robinson AC, Knight TJ, Durbin RD. 1987. Inactivation of pea seed glutamine synthetase by the toxin, tabtoxinine-beta-lactam. The Journal of Biological Chemistry **262**, 1608–1613.

Less H, Galili G. 2008. Principal transcriptional programs regulating plant amino acid metabolism in response to abiotic stresses. Plant Physiology **147**, 316–330.

Less H, Galili G. 2009. Coordinations between gene modules control the operation of plant amino acid metabolic networks. BMC Systems Biology **3**, 14.

Mahmood T, Woitke M, Gimmler H, Kaiser WM. 2002. Sugar exudation by roots of kallar grass [*Leptochloa fusca* (L.) Kunth] is strongly affected by the nitrogen source. Planta **214**, 887–894.

Mandon J, Mur LA, Harren FJ, Cristescu SM. 2016. Laser-based methods for detection of nitric oxide in plants. Methods in Molecular Biology **1424**, 113–126.

Morot-Gaudry-Talarmain Y, Rockel P, Moureaux T, Quilleré I, Leydecker MT, Kaiser WM, Morot-Gaudry JF. 2002. Nitrite accumulation and nitric oxide emission in relation to cellular signaling in nitrite reductase antisense tobacco. Planta **215**, 708–715.

Mur LA, Brown IR, Darby RM, Bestwick CS, Bi YM, Mansfield JW, Draper J. 2000. A loss of resistance to avirulent bacterial pathogens in tobacco is associated with the attenuation of a salicylic acid-potentiated oxidative burst. The Plant Journal **23**, 609–621.

Mur LAJ, Bi YM, Darby RM, Firek S, Draper J. 1997. Compromising early salicylic acid accumulation delays the hypersensitive response and increases viral dispersal during lesion establishment in TMV-infected tobacco. Plant Journal **12**, 1113–1126.

Mur LAJ, Mandon J, Cristescu SM, Harren FJ, Prats E. 2011. Methods of nitric oxide detection in plants: a commentary. Plant Science **181**, 509–519.

Mur LAJ, Mandon J, Persijn S, Cristescu SM, Moshkov IE, Novikova GV, Hall MA, Harren FJ, Hebelstrup KH, Gupta KJ. 2013a. Nitric oxide in plants: an assessment of the current state of knowledge. AoB PLANTS **5**, pls052.

Mur LAJ, Prats E, Pierre S, Hall MA, Hebelstrup KH. 2013b. Integrating nitric oxide into salicylic acid and jasmonic acid/ethylene plant defense pathways. Frontiers in Plant Science **4**, 215.

Mur LAJ, Simpson C, Kumari A, Gupta AK, Gupta KJ. 2017. Moving nitrogen to the centre of plant defence against pathogens. Annals of Botany **119**, 703–709.

Patterson K, Walters LA, Cooper AM, Olvera JG, Rosas MA, Rasmusson AG, Escobar MA. 2016. Nitrate-regulated glutaredoxins control Arabidopsis primary root growth. Plant Physiology **170**, 989–999.

Planchet E, Sonoda M, Zeier J, Kaiser WM. 2006. Nitric oxide (NO) as an intermediate in the cryptogein-induced hypersensitive response–a critical re-evaluation. Plant, Cell & Environment **29**, 59–69.

Prats E, Mur LA, Sanderson R, Carver TL. 2005. Nitric oxide contributes both to papilla-based resistance and the hypersensitive response in barley attacked by *Blumeria graminis* f. sp. *hordei*. Molecular Plant Pathology **6**, 65–78.

Singh SK, Chien CT, Chang IF. 2016. The Arabidopsis glutamate receptor-like gene *GLR3.6* controls root development by repressing the Kip-related protein gene *KRP4*. Journal of Experimental Botany **67**, 1853–1869.

Solomon PS, Oliver RP. 2001. The nitrogen content of the tomato leaf apoplast increases during infection by *Cladosporium fulvum*. Planta **213**, 241–249.

Vaucheret H, Kronenberger J, Lepingle A, Vilaine F, Boutin JP, Caboche M. 1992. Inhibition of tobacco nitrite reductase activity by expression of antisense RNA. The Plant Journal **2**, 559–569.

Walch-Liu P, Liu LH, Remans T, Tester M, Forde BG. 2006. Evidence that L-glutamate can act as an exogenous signal to modulate root growth and branching in *Arabidopsis thaliana*. Plant & Cell Physiology **47**, 1045–1057.

Wang R, Guegler K, LaBrie ST, Crawford NM. 2000. Genomic analysis of a nutrient response in Arabidopsis reveals diverse expression patterns and novel metabolic and potential regulatory genes induced by nitrate. The Plant Cell **12**, 1491–1509.

Wang R, Tischner R, Gutiérrez RA, Hoffman M, Xing X, Chen M, Coruzzi G, Crawford NM. 2004. Genomic analysis of the nitrate response using a nitrate reductase-null mutant of Arabidopsis. Plant Physiology **136**, 2512–2522.

Wang R, Xing X, Crawford N. 2007. Nitrite acts as a transcriptome signal at micromolar concentrations in Arabidopsis roots. Plant Physiology **145**, 1735–1745.

Xia J, Sinelnikov IV, Han B, Wishart DS. 2015. MetaboAnalyst 3.0–making metabolomics more meaningful. Nucleic Acids Research **43**, W251–W257.

Xu N, Wang R, Zhao L, *et al.* 2016. The Arabidopsis NRG2 protein mediates nitrate signaling and interacts with and regulates key nitrate regulators. The Plant Cell **28**, 485–504.

Yoshida R, Mori IC, Kamizono N, Shichiri Y, Shimatani T, Miyata F, Honda K, Iwai S. 2016. Glutamate functions in stomatal closure in Arabidopsis and fava bean. Journal of Plant Research **129**, 39–49.

Zeidler D, Zahringer U, Gerber I, Dubery I, Hartung T, Bors W, Hutzler P, Durner J. 2004. Innate immunity in *Arabidopsis thaliana:* lipopolysaccharides activate nitric oxide synthase (NOS) and induce defense genes. Proceedings of the National Academy of Sciences, USA **101**, 15811–15816.

Zeier J, Delledonne M, Mishina T, Severi E, Sonoda M, Lamb C. 2004. Genetic elucidation of nitric oxide signaling in incompatible plant-pathogen interactions. Plant Physiology **136**, 2875–2886.